Plasmonics (2016) 11:1019–1024
DOI 10.1007/s11468-015-0137-6

Near-Infrared Absorption Enhancement Mechanism Investigations of Deep-Trench Silicon Microstructures Covered with Gold Films

Xiaoyi Liu [1,2] · Jinsong Gao [1,2] · Haigui Yang [2] · Hai Liu [2] · Xiaoyi Wang [2] · Zhenfeng Shen [2]

Received: 27 August 2015 / Accepted: 2 November 2015 / Published online: 14 November 2015

Abstract We design a deep-trench microstructure covered with thin gold films to enhance near-infrared absorption of silicon material. This deep-trench microstructure exhibits a much higher absorption compared with plane nanoantenna arrays. We investigate its absorption enhancement in detail and find that the trench-shaped plasmonic waveguide greatly contributes an absorption enhancement by concentrating light effectively. Further, we clarify the influence of both trench depth and gold films covering on different positions of deep trench on the absorption. Finally, we use surface plasmon polaritons offered by plasmonic waveguide to explain well the significant enhancement of near-infrared absorption.

Keywords Near-infrared absorption · Deep-trench microstructure · Plasmonic waveguide · Surface plasmon polaritons

Introduction

Among all optoelectronic devices, silicon-based devices are the most widely used because of their outstanding merits such as low cost, high performance, mature technology, etc. But due to their wide band gap (1.12 eV), the response range of silicon-based optoelectronic devices focuses on the visible spectrum mainly. It has no response on the near-infrared (NIR) light with the wavelengths greater than 1200 nm, which severely limits their applications in the NIR band. Now, the optoelectronic devices of the NIR band are mainly using Ge, InGaAs, and other compound materials, but these devices have some shortcomings such as high cost, poor stability, and complex process. Therefore, much attention is still paid to improve the NIR light absorption of silicon-based materials to extend their response range into the NIR region. In order to realize this purpose, researchers have proposed several methods. For example, some research teams used the fs-laser processing technology to process a microstructure surface with a cone-shaped structure arranged in an array [1, 2]. The more important thing is that the high-energy fs-laser would inject the supersaturated doping ion into silicon surface, resulting in an improving absorption of the NIR light to extend the NIR response of silicon optoelectronic devices [3–6]. Other research groups produced dot or rectangle metal nanoantenna arrays on silicon surface [7–9], by which the excited surface plasmon polaritons (SPPs) enhance the absorption of NIR light, while the hot electrons generated by non-radiative decay of SPPs pass through a Schottky barrier at the metal/silicon interface into silicon conduction band; thereby, it forms photocurrents to extend the NIR response of silicon optoelectronic devices. However, this method has some weaknesses such as small structural unit size, high-cost lithography process, limitation to improve the absorption etc. Very recently, Lin et al. have proposed a novel deep-trench microstructure covered with a layer of gold film on silicon substrate [10]. This structure induces a cavity effect to enhance silicon absorption of NIR light greatly, which is ten times higher than that by nanoantenna structures [10]. In addition, the size of this deep-trench structure is large and consequently easy to be fabricated; thus, this structure has great applied potential. But so far, the further mechanism and decisive factors of infrared

✉ Haigui Yang
yanghg@ciomp.ac.cn

[1] University of the Chinese Academy of Sciences, Beijing 100039, China

[2] Key Laboratory of Optical System Advanced Manufacturing Technology, Changchun Institute of Optics, Fine Mechanics and Physics, Chinese Academy of Sciences, Changchun 130033, China

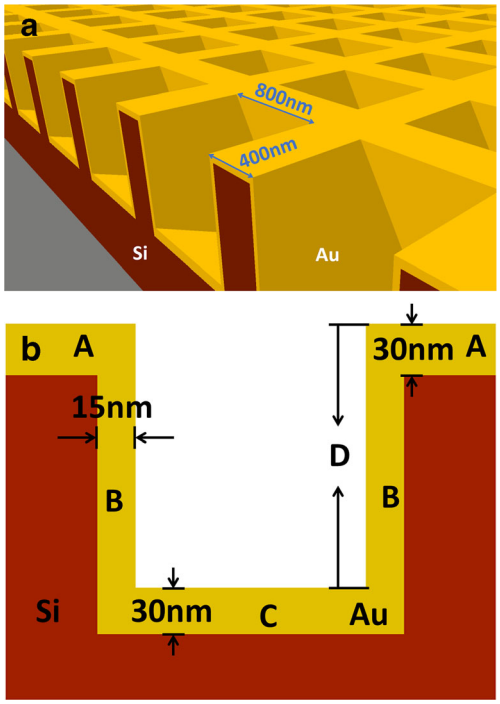

Fig. 1 **a** Three-dimensional model diagram of deep-trench microstructure; **b** Cross-sectional diagram of an unit of deep-trench microstructure

light absorption enhancement generated in the deep-trench microstructure of silicon are still not clarified.

In this study, we design a deep-trench Si-based microstructure covered with gold films and discuss the distributions of electric field intensity (E) in the deep trench and the influence of trench depth on the NIR absorption in detail. We use a plasmonic waveguide model to explain the simulation results. Further, we discuss the influences of the different parts of the gold film covering on the deep trench on E to clarify the contributions of trench-shaped microstructures on the significant enhancement in NIR absorption.

Modeling Calculation

A three-dimensional finite difference-time domain (3D-FDTD) method is used to make a simulation study on the deep-trench Si-based microstructure covered with gold films. The three-dimensional and cross-sectional diagrams of microstructure are given in Fig. 1a, b, respectively. The microstructure of silicon surface is composed of periodically arranged square trenches, whose side length is 0.8 μm, period is 1.2 μm, and depth is D as a variable parameter. The top of the microstructure surface and the bottom and sidewalls of the

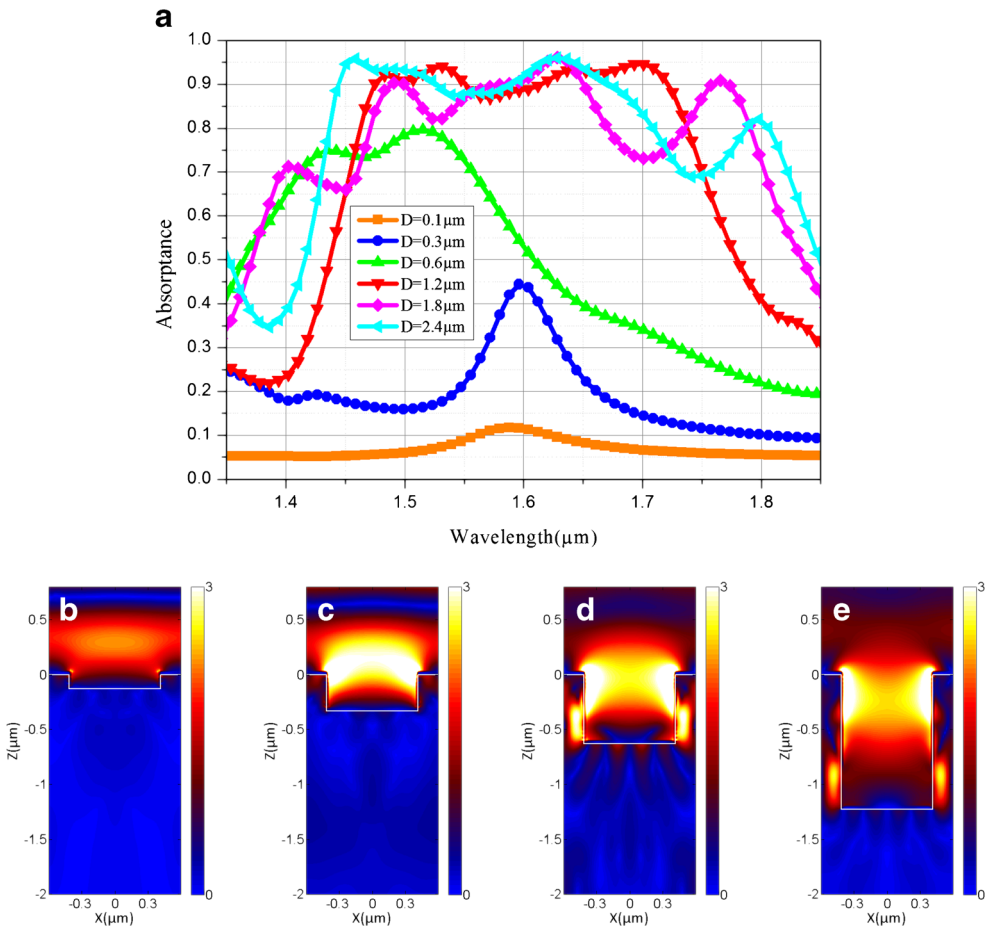

Fig. 2 **a** The dependence of different depths (D) of trench microstructures on near-infrared (NIR) light absorption. The vertical axis is simulated absorptance (A). **b**, **c**, **d**, **e** Electric field intensity (E) distribution diagrams of trench microstructures with different trench depths (D) when the incident wavelength is 1.5 μm. The depths are 0.1, 0.3, 0.6, and 1.2 μm, respectively. The polarization direction of the incident light is along the X axis, and the color bars (a.u.) are consistent

deep trench are covered with a layer of gold film. The gold film thickness on both top and bottom is 30 nm, and the sidewall is 15 nm. The designed deep-trench surface microstructure covered with gold films has two advantages: One is that SPPs can be excited at the metal microstructure surface [11–15] to enhance the absorption of NIR light; Another is that by using this structure to prepare photoelectric detectors, a large area of gold films on the surface can be acted as metal electrodes, which helps contribute greatly to the extraction of photocurrent [9, 10].

Results

Figure 2a shows the influence of D on NIR light absorption, and the vertical axis is simulated absorptance (A). From Fig. 2a, it can be seen that the absorption enhancement in NIR light is strongly dependent on D. When D=0.1 μm, the absorption of NIR light is enhanced, but its effect is very limited, and this situation is similar to nanoantennas [10]. However, with an increase in D, the absorption of NIR light dramatically increases. When D goes to 1.2 μm, A is saturated. The average A in the wavelength range from 1.5 to 1.7 μm is as high as 90 %, and its peak reaches 95 %.

In order to explain the influence of D on the absorption, we drew E distribution diagrams of the trench microstructure with different D when the incident wavelength is 1.5 μm, shown in Fig. 2b-e. The polarization direction of the incident light is along the X axis. Figure 2b-e shows the E distributions when D=0.1, 0.3, 0.6, and 1.2 μm, respectively. The color bars are consistent, and the highlighted areas show that E is greater than others. It is worth noting that the energy in the cavity is not evenly distributed but mainly concentrated in the vicinity of two vertexes and side walls, similar to the results in the reports of Ma et al. [15], Li et al. [16], and Zhu et al. [17]. With an increase in D, the binding effect from the deep trench on the electric field becomes obvious increasingly. This energy distribution should have a very important influence on the high absorption of NIR light. Significant absorption enhancement in NIR light and the dependence of E on D mentioned above should be attributed to the trench-shaped waveguide. Zhu et al. have introduced a simple and efficient method to realize on-chip plasmon-induced transparency in a trench-shaped plasmonic waveguide [17]. In their report, the trench-shaped plasmonic waveguide can offer wideband guided SPP modes. The energy is mainly confined in the nanocavity and distributed around two vertexes of the nanocavity [17].

Figure 3a shows the top-view E distributions in the depth of 0.25 μm for the deep trench with D=1.2 μm at the wavelength of 1.5 μm. The polarization direction of the incident light is along the X axis. Obviously, the energy near the upper sidewalls is greatly concentrated. As shown in Fig. 2b-e and Fig. 3a, near the gold films on both upper sidewalls of deep

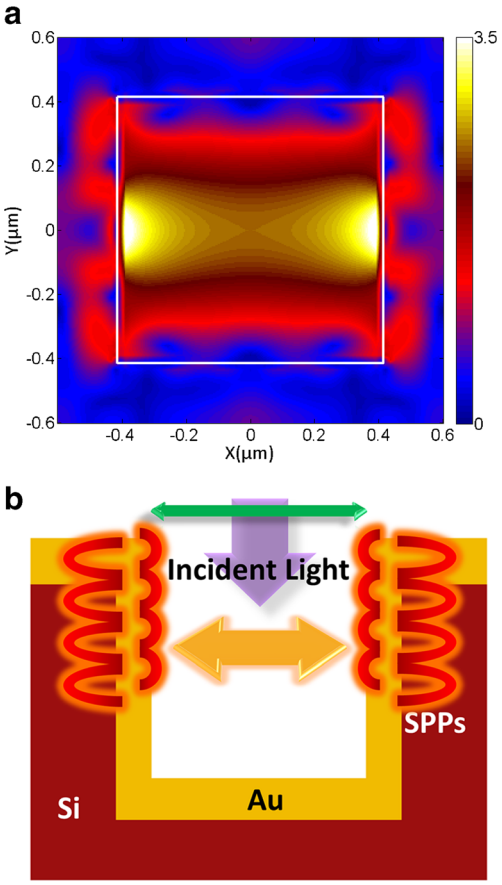

Fig. 3 **a** Top-view electric field intensity (E) distribution in the depth of 0.25 μm of the deep-trench microstructure at the wavelength of 1.5 μm. The trench depth (D) is 1.2 μm. The polarization direction of the incident light is along the X axis. **b** The process diagram that the incident light energy is gathered and transferred by surface plasmon polaritons (SPPs) offered by plasmonic waveguide

trenches, a large number of SPPs are generated and subsequently transfer the energy of incident light in the cavity. Figure 3b shows the process diagram of the incident light

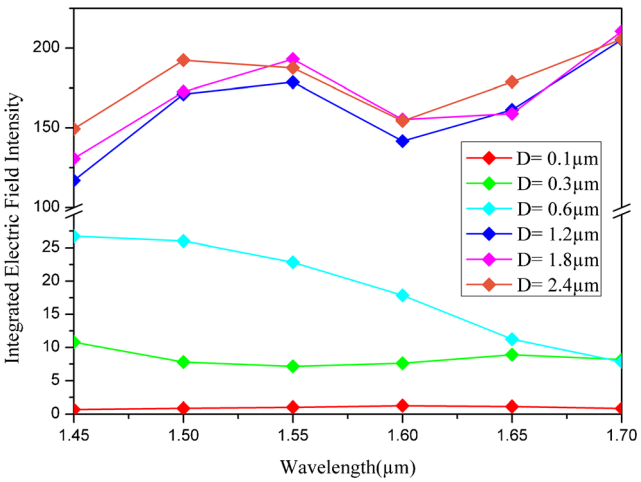

Fig. 4 The dependence of integrated electric field intensities (integrated E) on different depths (D) of trench microstructures. The electric field intensity is integrated along the side walls of trench microstructures

energy gathered and transferred through SPPs offered by plasmonic waveguide. This plasmonic waveguide structure plays a role that generates SPPs rather than transmits them reported in Refs. [18] and [19]. Significant enhancement in NIR absorption is originated from the impact including all above processes. As a result, the converging light energy in the deep trench is constantly coupled to the SPPs; leading to that, both the reflection and transmission of NIR light are drastically reduced, and consequently NIR absorption is significantly enhanced. Moreover, the wideband SPPs offered by the plasmonic waveguide [17, 20] is the reason why the spectrum region of high absorption is so large (1.5–1.7 μm). Compared with the report of Lin et al. [10], we achieved a wider spectrum with a higher absorption by optimization and most importantly clarified the mechanism and decisive factors of NIR absorption enhancement in detail.

Discussion

Efficient absorption of NIR light needs SPPs excited by the plasmonic waveguide structures that confined energy near the two vertexes of the cavities shown in Fig. 2b-e and Fig. 3a, from which we can explain well that why *A* is saturated when

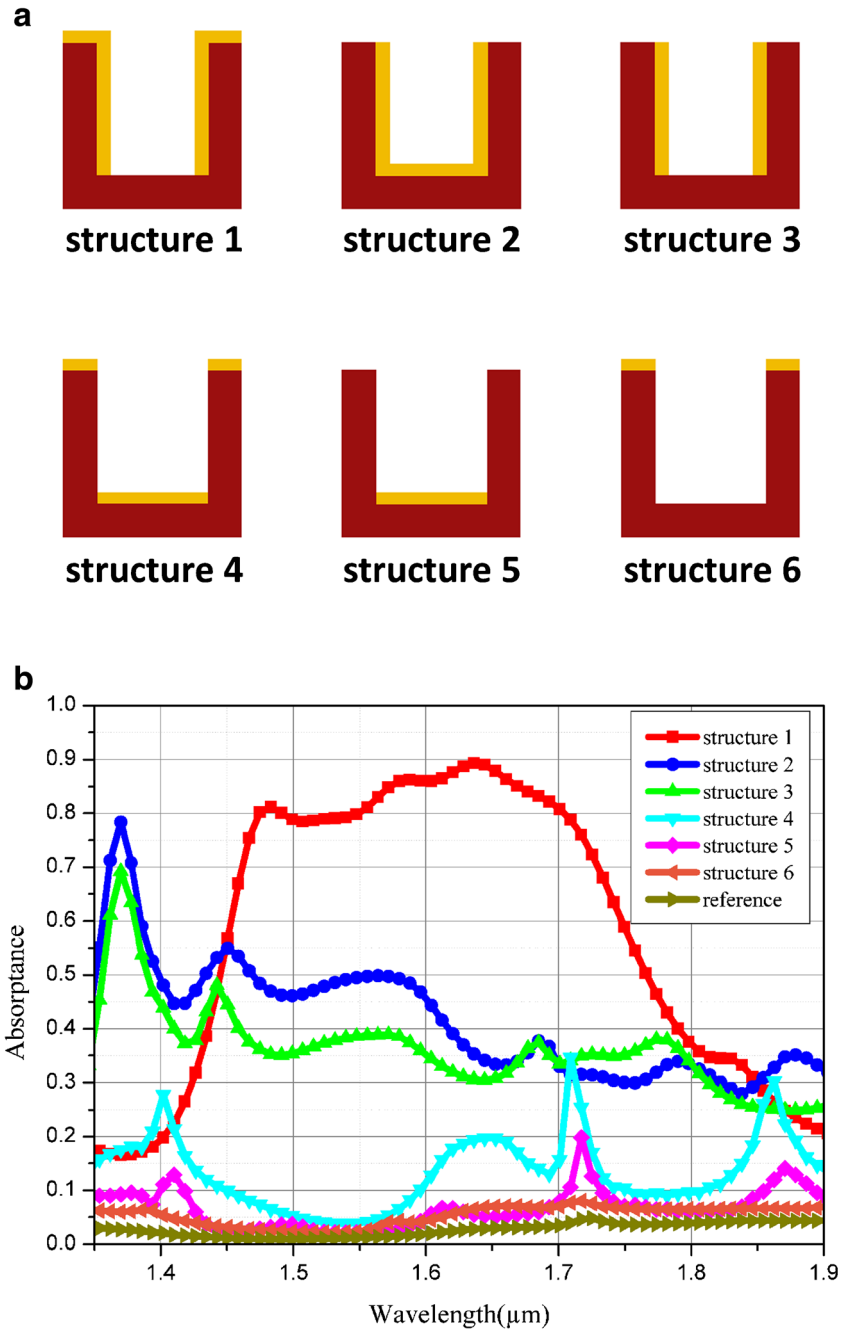

Fig. 5 **a** Cross-sectional diagrams of deep-trench microstructures with different part gold films. **b** Near-infrared absorptances of structure 1~6. The vertical axis is simulated absorptance (*A*). The reference curve belongs to a structure without any gold film

D goes over 1.2 μm in Fig. 2a. When D is large enough to contain the concentrated energy near vertexes, further increasing D will be less effect on NIR absorption enhancement. To verify this consideration, we make E values along the side walls into a line integral, and give the dependence of integrated E on D in Fig. 4. In a range of wavelength from 1.45 to 1.7 μm, the integrated E increases with the increase of D. Especially when D=1.2 μm, its value is more than 100, much larger than the former three, and about an order of magnitude higher than the average integrated E for the trench with D= 0.6 μm. But when D continues to increase, the enhancement of the integrals is not obvious. This result shows a good agreement with the conclusion above.

In the following, we analyzed the impact of the gold films in different locations in the deep trench on NIR absorption. Here, we divide gold films into three parts: the top of the microstructure, the bottom of the trench, and sidewalls, corresponding to A, B, and C in Fig. 1b. Figure 5a shows the cross-sectional microstructures with different part gold films at D= 1.2 μm. We conducted a simulation of these structures and got their simulated A of NIR light shown in Fig. 5b.

From Fig. 5b, we can see some interesting information. The structure 1 gets the highest A in a wavelength range from 1.5 to 1.7 μm, reaching more than 80 %. Two absorption curves in the middle belong to structure 2 and 3. Their average absorptances remain at around 40 %, respectively. The common point of structure 1, 2, and 3 is that their trench sidewalls are all under cover of gold films. In contrast, the absorptances of the structure 4, 5, and 6 are very low. The common point of them is the lack of gold films covering on the trench sidewalls, which means gold films covered on the deep-trench sidewalls have the significant contribution to NIR absorption. Compared with other parts, the gold films covered on sidewalls are the foundation of high absorption. In addition, we noticed that the absorptance of structure 1 is two times higher than that of structure 2 and 3. We believed that it is because the gold films covered on the top surface of microstructures can improve the efficiency of exciting SPPs. The contribution of SPPs generated by the large-area gold films covered on the top surface to improving the absorption is not negligible. As for the existence of relatively sharp peaks in absorption curves of structure 2~5, we considered that they are caused by the higher-order SPP modes [21].

Figure 6 shows E distributions of structure 1~6 in Fig. 5a at the wavelength of 1.5 μm. The polarization direction of the incident light is along the X axis, and the color bars are consistent. By comparison, we can see that the gold films on the trench sidewalls have the most important impact on E

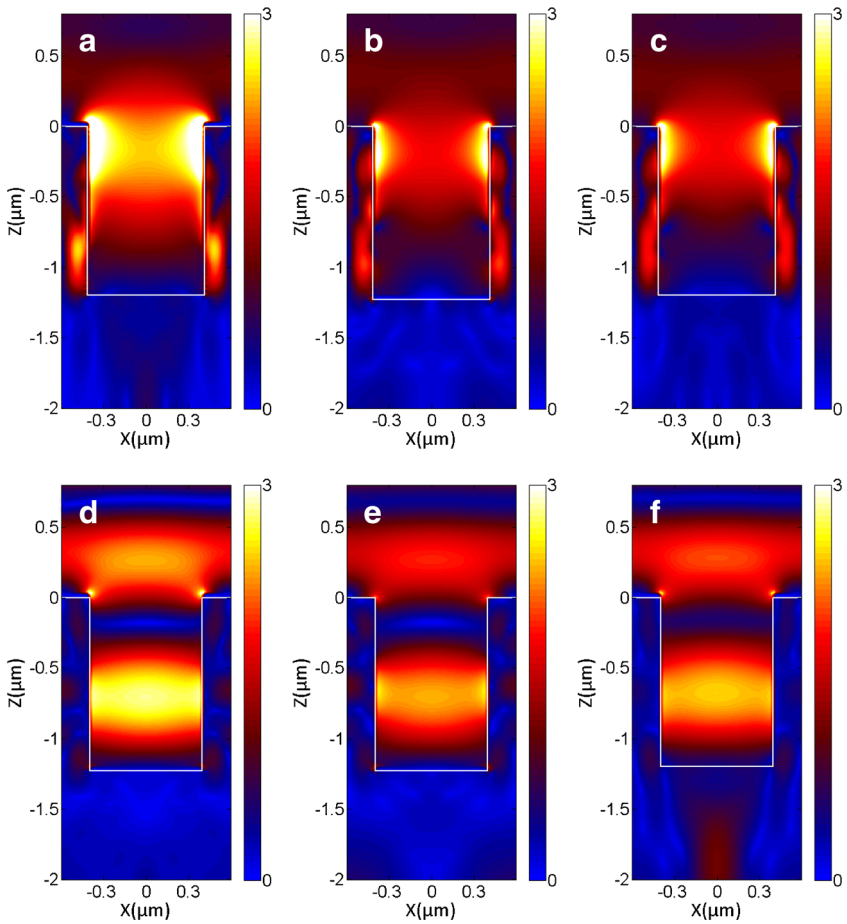

Fig. 6 **a**, **b**, **c**, **d**, **e**, **f** Electric field intensity (E) distributions of structure 1~6 at the wavelength of 1.5 μm. The polarization direction of the incident light is along the X axis, and the color bars (a.u.) are consistent

distributions. For the structure 1, 2, and 3 all with gold films covering on the sidewalls, the electric field energy is concentrated closely on the upper sidewalls, but for the structure 4, 5, and 6 without the gold films covering on the sidewalls generally do not have such a characteristic, by which it is confirmed clearly that the gold films covering on the sidewalls are indispensable to the plasmonic waveguide. Moreover, other group has reported that standing waves were formed in different modes between both sides of a gold trench, by which the energy redistribution in the cavity can be controlled [22]. This also indicates the importance of the gold films on the sidewalls.

Conclusion

In summary, we have successfully demonstrated a significant enhancement of near-infrared light absorption in silicon material by using a deep-trench microstructure covered with gold films. We found that the SPPs induced in the deep trench contribute an absorption enhancement by concentrating the light effectively, and gold films covering on the trench sidewalls have the most significant contributions on the NIR absorption compared with other parts. The highest average absorptance of deep-trench covered with gold films was as high as 90 %, and its peak reached 95 % in the wavelength range from 1.5 to 1.7 μm. Due to the SPPs offered by plasmonic waveguide that can transfer the incident light energy, the deep-trench microstructures covered with gold films achieved a significant enhancement of near-infrared light absorption. By the deep-trench structures, we provided a promising approach to extend silicon-based optoelectronic devices to the near-infrared region.

Acknowledgments This project was supported by the National Natural Science Foundation of China (Nos. U1435210 and 61306125), the Science and Technology Innovation Project (Y3CX1SS143) of CIOMP, the Science and Technology Innovation Project of Jilin Province (nos. Y3293UM130, 20130522147JH and 20140101176JC).

References

1. Huang ZH, Carey JE, Liu MG, Guo XY, Mazura E, Campbellb JC (2006) Microstructured silicon photodetector. Appl Phys Lett 89: 033506
2. Kalem S, Werner P, Arthursson Ö, Talalaev V, Nilsson B, Hagberg M, Frederiksen H, Södervall U (2011) Black silicon with high density and high aspect ratio nanowhiskers. Nanotechnology 22:235307
3. Smith MJ, Sher MJ, Franta B, Lin YT, Mazur E, Gradečak S (2014) Improving dopant incorporation during femtosecond-laser doping of Si with a Se thin-film dopant precursor. Appl Phys A 114:1009
4. Younkin R, Carey JE, Mazur E, Levinson JA, Friend CM (2003) Infrared absorption by conical silicon microstructures made in a variety of background gases using femtosecond-laser pulses. Appl Phys 93:2626
5. Crouch CH, Carey JE, Shen M, Mazur E, Génin FY (2004) Infrared absorption by sulfur-doped silicon formed by femtosecond laser irradiation. Appl Phys A 79:1635
6. Wang YL, Liu SY, Wang Y, Feng GJ, Zhu JT, Zhao L (2009) Infrared light absorption of silver film coated on the surface of femtosecond laser microstructured silicon in SF_6. Mater Lett 63: 2718
7. Knight MW, Sobhani H, Nordlander P, Halas NJ (2011) Photodetection with active optical antennas. Science 332:702
8. Sobhani A, Knight MW, Wang YM, Zheng B, King NS, Brown LV, Fang ZY, Nordlander P, Halas NJ (2013) Narrowband photodetection in the near-infrared with a plasmon-induced hot electron device. Nat Commun 4:1643
9. Li W, Valentine J (2014) Metamaterial perfect absorber based hot electron photodetection. Nano Lett 14:3510
10. Lin KT, Chen HL, Lai YS, Yu CC (2014) Silicon-based broadband antenna for high responsivity and polarization-insensitive photodetection at telecommunication wavelengths. Nat Commun 5:3288
11. Akimov YA, Ostrikov K, Li EP (2009) Surface plasmon enhancement of optical absorption in thin-film silicon solar cells. Plasmonics 4:107
12. Karpinski P, Miniewicz A (2011) Surface plasmon polariton excitation in metallic layer via surface relief gratings in photoactive polymer studied by the finite-difference time-domain method. Plasmonics 6:541
13. Zavareian N, Massudi R (2012) Localization of light with two metallic wedges: a step toward surface plasmon sources. Plasmonics 7: 447
14. Vashchenko EV, Vartanyan TA, Hubenthal F (2013) Photoconductivity of silver nanoparticle ensembles on quartz glass (SiO_2) supports assisted by localized surface plasmon excitations. Plasmonics 8:1265
15. Ma A, Li Y, Zhang XP (2013) Coupled mode theory for surface plasmon polariton waveguides. Plasmonics 8:769
16. Li XE, Jiang T, Shen LF, Deng XH (2013) Subwavelength guiding of channel plasmon polaritons by textured metallic grooves at telecom wavelengths. Appl Phys Lett 102:031606
17. Zhu Y, Hu XY, Yang H, Gong QH (2014) On-chip plasmon-induced transparency based on plasmonic coupled nanocavities. Sci Rep 4:3752
18. Wu T, Liu Y, Yu Z, Ye H, Shu C, Peng Y, Zhang W, Wang J, He H (2015) Tuning the Fano resonances in a single defect nanocavity coupled with a plasmonic waveguide for sensing applications. Optik, DOI:10.1016.
19. Yu HB, Sun C, Tang HY, Deng XX, Li JH (2014) A surface-plasmon-polariton wavelength splitter based on a metal–insulator–metal waveguide. Photonics Nanostruct 12:460
20. Wu KY, Rindzevicius T, Schmidt MS, Mogensen KB, Xiao SS, Boisen A (2015) Plasmon resonances of Ag capped Si nanopillars fabricated using mask-less lithography. Opt Express 23:12965
21. Hooper IR, Sambles JR (2002) Dispersion of surface plasmon polaritons on short-pitch metal gratings. Phys Rev B 65:165432
22. Qiao M, Gordon R (2008) Surface plasmon microcavity for resonant transmission through a slit in a gold film. Opt Express 16:9708